A Comparative Study on the Performance of Hidden Markov Model in Appliance Modeling

Hebatullah M. Malik
Electrical and Computer Engineering
Effat University
Jeddah, Saudi Arabia
e-mail: hemalik@effat.edu.sa

Nema Salem
Electrical and Computer Engineering
Effat University
Jeddah, Saudi Arabia
e-mail: nsalem@effatuniversity.edu.sa

Maha S. AlSabban
Electrical and Computer Engineering
Effat University
Jeddah, Saudi Arabia
e-mail: maalsabban@effat.edu.sa

***Abstract*—Load modeling using data-driven algorithms is a widely used technique in applications like load identification. It is also one of the fundamental concepts which enable Non-Intrusive Appliance Load Modeling (NIALM). This paper develops a load modeling framework using Hidden Markov Models (HMMs) to identify a two-state home appliance. Unlike previous studies, the training and testing dataset is derived from different monitored domestic houses to analyze the effect of the training data trends on the model's accuracy. We used the Reference Energy Disaggregation Dataset (REDD) in the load modeling process. The developed system utilizes adaptive measures to construct HMM models that can identify foreign variants of the same two-state appliance. We measured the accuracy of our proposed methodology by comparing a known state sequence with a Viterbi-generated one. The accuracy results are up to 96%, depending on the nature of the used training dataset.**

Keywords-adaptation; appliance identification; data analysis; finite state-machine; hidden Markov model; power consumption

I. INTRODUCTION

Non-Intrusive Appliance Load Modeling (NIALM) was first introduced in the 1980s to disaggregate the total power consumption of a residential unit into its basic components (i.e., individual electric circuits) [1]. The technology proved its ability to identify and track the electricity consumption and infer the status of appliances, which has enabled buildings' efficiency endeavors. Researchers in [2] claimed that 10-15% of power consumption can be eliminated using energy management principles. Such principles can only be deduced after being able to study patterns through technologies similar to NIALM.

Residential buildings specifically use up a considerable share of the net annually generated power. In 2017, Saudi Arabia's residential share surmounted its industrial, commercial, and governmental sectors combined [3]. There arises the need to adopt feasible and relatively fast solutions to achieve energy efficiency goals established by the country. This includes sanctioning new laws and tariffs as well as raising consumer awareness on their electricity usage to enable them to make sustainable decisions. NIALM plays an important role in assisting household members in monitoring their regular electricity consumption. Therefore, it is important to study some of the methodologies used to realize NIALM. This includes intelligent methods (using deep learning networks or others) or via statistical approaches such as Hidden Markov Models (HMM).

HMM, which is based on Markov chain principles, has been renowned for its use in speech recognition and biological applications [1], [4]. However, the applicability of HMM has further expanded its realm to include other fields such as electrical load modeling. HMM has helped researchers represent/model electric appliances stochastically from their recorded power consumption. This is possible due to Markov chains' main feature in which it affirms that a future state at t + 1 (one step) is dependent only on the current state at t without considering other previous states. This application was instrumental and fundamental in the insurgence of NIALM where the recorded data can become lengthy.

This paper studies the efficacy of HMM in modeling two-state appliances such as lamps, and toasters. First, a step-by-step approach is presented on how to build an HMM model for a single appliance, and later on, adapt it to use variants to model an unknown appliance of the same type. Second, a test scheme is developed and the accuracy is measured to compare the results and draw a conclusion. The paper shall serve as a guide for researchers who need to measure the performance of HMM separately from the application of NIALM.

II. LITERATURE REVIEW

This section reviews several works related to appliance modeling using HMM. Most of the presented studies concentrated solely on building and evaluating models for individual appliances using HMM, while other studies incorporated additional algorithms to either improve the performance of the models or to realize more complex goals such as combined loads disaggregation (NIALM).

In [5], the authors acquired a unique active power consumption dataset for six different appliances with a 10-second sampling rate. They utilized Finite State-Machine FSM to dictate the different states of a target appliance and found the HMM model (λ) for it. To verify the calculated model, the authors fed the model to a Viterbi algorithm to generate a power signal for the studied appliance. However, the study lacked quantitative analysis to draw comparisons between the two signals (original against Viterbi-generated).

Authors in [6] utilized a combination of data generated from their own lab setup, and the online Tracebase appliances repository [7] (both measuring active power at a one-second sampling rate) to find individual load models for eight appliances. Similar to [5], the FSM of each appliance was found manually. This study fortified the robustness of their individual HMM models through the use of appliance variants. Meaning that each HMM load model (λ) was generated from averaging four different variants of a certain appliance. To verify their model, the authors used the averaged models of each appliance as an input to a Viterbi algorithm to predict the power signal of a fifth unknown variant for the five-second sample and the 30-second sample. This was done five times for each appliance with changing the unknown variant each time. The authors then used k-fold cross-validation to find the correlation between the calculated Viterbi and the original observation data of that unknown variable (five correlation values per appliance), then averaged the correlations per appliance. The correlation results range was (70.75% – 99.63%) for the five-second sampled Viterbi, and (32.35% – 97.14%) for the 30-second sampled Viterbi. A study conducted by [8] utilized an adapted HMM methodology to build versatile mathematical models for eight appliances derived from the UKDALE dataset. The purpose of the adapted HMM models was to accommodate consumption changes across appliances of different brands. The study extracted the active power consumption throughout 16 hours; however, the authors did not specify whether the duration was continuous or intermittent. Moreover, the study implemented Expectation-Maximization (EM) algorithms to estimate the states of each appliance, unlike previously presented studies that defined the states manually. After the models were constructed, Akaike Information Criterion (AIC) was used to evaluate the fitness of the models. The results showed that the HMM models fitted controlled state appliances such as toasters better than uncontrolled state appliances like fridges. However, we noticed that this work lacked vigorous analysis and discussion of their results which may have led to misinterpretation of their findings. Sankara [9] utilized the same modeling principle as [6], which was to find an appliance model (λ) through averaging multiple variants. The individual models were built using the Tracebase repository, and K-fold cross-validation was used to determine the accuracy of each model's generated Viterbi sequence against a known observation sequence. The correlation results showed that higher correlations were observed at fast-sampling rates (95% at five-second sampling rate) compared to low-sampling rates (85% at 15-minute sampling rate). Nandy [10] further contributed to the literature by proposing an HMM load model that considers both active and reactive power consumed by an appliance to find a Viterbi sequence. The accuracy was found using the correlation coefficient for models of an oven, a dryer, a microwave, and a cooling/heating. The correlation coefficient showed that the proposed method was more effective in modeling appliances. It increased from 0.5157 to 0.9642 for the oven, 0.7784 to 0.9936 for the dryer, and from 0.6668 to 0.9675 for the cooling/heating device; but it slightly dropped down from 0.9349 to 0.9128 for the microwave. An improved HMM called the conditional Hidden Semi-Markov Model (HSMM) was constructed in [11] to relate the state transitions to environmental factors such as time and temperature. The model's complexity increased from three parameters to five and thus required alternative methodologies to obtain the conditional HSMM model such as K-means clustering and multinomial logistic regression. However, instead of assessing the accuracy of the generated model against a test dataset, the proposed algorithm was evaluated in an active-power forecasting application. The authors trained their model on five appliances, 20 variants for each appliance, with a training set of five months in length. The forecasting algorithm was then tested for a duration of one month. For this month, the algorithm predicted the next six hours with a 15 minutes resolution (four values per hour). The dataset used was the Pecan Street database [12]. The authors evaluated their forecasting algorithm using Root-Mean-Square Error RMSE and Normalized Root-Mean-Square Error NRMSE for each appliance (the calculated values were averaged over 20). To show the impact of the conditional HSMM model, the performance metrics were compared to those of a conventional HSMM model for the same dataset. The conditional HSMM appeared to be superior to its counterpart in all appliances which confirms the efficacy of the upgraded model

III. Proposed Methodology

This section discusses the steps and techniques required to achieve an HMM for an individual appliance, namely a lamp.

To construct an HMM model for an individual appliance using its states, two main procedures are followed:

1) Structure modeling.
2) Parameters estimation.

Structure modeling is completed in two stages. First, the number of the total states of the appliance must be determined. The states are identified by the complete set of distinct power levels an appliance consumes. Second, the topology in which the distinct states interact must be specified.

Two topologies describe states' interactions: left-right topology, and ergodic topology. Left-right topology allows its state transition to move only from left to right as time progresses [5]. However, ergodic topology allows states to transition freely to a new or a previous state as time progresses. Fig. 1 illustrates the possible interaction scenarios in each topology.

After structuring the model, the parameters estimation procedure begins. There are several approaches to estimate un- known parameters. The prevalent approaches are the forward-backward, Baum-Welch, Viterbi, and EM algorithms [13], [14]. Every algorithm is used with specific sets of data and has different advantages and disadvantages. However, the model parameters (λ) in this study were calculated using probability functions. Moreover, the Viterbi algorithm was utilized to verify our calculated model.

The previously mentioned procedures are applied to a lamp. Its structure consists of only two distinct states: ON,

and OFF. The state-transition diagram of a lamp forms an ergodic topology as shown in Fig. 2. The calculation of the unknown parameters in a lamp's HMM is explained in the next sub-section.

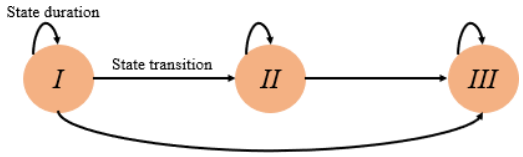

(a) Left-right topology.

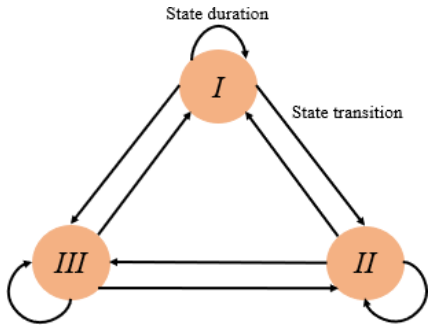

(b) Ergodic topology.

Figure 1. Commonly used topologies to describe states' interactions in HMM.

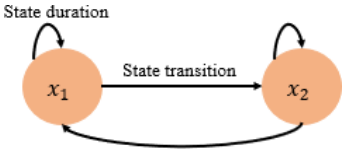

Figure 2. The complete set of state interactions for a lamp; x_1= OFF state, and x_2= ON state.

A. Calculating Model Parameters:

The HMM model is defined as λ = (π, A, B) where A is the transition matrix, B is the emission probability matrix, and π is the initial probability matrix.

The created lamp model created has a set of states $X = \{x_1, x_2\}$ with a number of states $N = 2$. This results in a transition matrix of size $N \times N$ as illustrated in Fig. 3a. To visualize what each probability means, a diagram is provided in Fig. 3b. To calculate the transition from one state to another (i.e., a_{ij}), (1) is used. The resulting matrix can be verified using (2) which states that the sum of the probabilities of transitioning from any state a_i (sum of elements in a single row) must equal one.

$$a_{ij} = P\,(X_{t+1} = j \mid X_t = i)\; i, j \in N \tag{1}$$

$$\Sigma^{N}_{j=1}\, a_{ij} = 1;\; i \in N \tag{2}$$

The emission matrix B represents the probability of making a certain observation at a given state. In our case, this means observing a certain power reading (in Volt-Amperes (VA)) at either state. However, due to the nature of lamps, which are linear devices that only consume active power (in Watts), their power consumption is referred to in Watts and not VA. The emission matrix B is easily obtained in our study compared to other applications because, in electric appliances, a unique power value can only exist in one state. For example, a lamp can never be turned on while consuming zero Watt, because zero Watt indicates an OFF state only. Therefore, a threshold value is manually set to stratify power observations to N number of groups as shown in Fig. 4. After segregation is done, the B matrix is calculated using (3) which states that $b(i,k)$ is the probability of observing o_k at state x_i. Given a series of unique observations $O = \{o_1, o_2, \ldots, o_K\}$ with a dimension $1 \times K$ each power value has a probability of appearing only in one of the states of the appliance. As the dimension of the B matrix must be $N \times K$, zeroes must be placed at the probability of a power value being observed out of its designated state. Fig. 5 illustrates the relationship between the states and the observations. To complete this model, an initial probability vector π is determined that states the probability of each state at time-step zero. We set this to be π = [x_1 = 0, x_2 = 1] to match the nature of our datasets. The sum of the π vector should always equal one.

$$b(i,k) = (\text{count}\,(o_k) \mid x_i) \div (\text{count}\,(o) \mid x_i) \tag{3}$$

$$A = \overbrace{\begin{pmatrix} a_{11} & a_{12} \\ a_{21} & a_{22} \end{pmatrix}}^{X_{t+1}} \Big\} X_t$$

(a) Transition matrix of a two-state appliance with the rows presenting the state at the current time step (t) and the columns presenting the state at the next time step (t + 1).

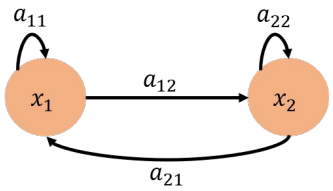

(b) Transition diagram of a lamp with probabilities.

Figure 3. Transition state matrix and diagram of a lamp where the diagram illustrates the placement of each probability with respect to the arrows' directions.

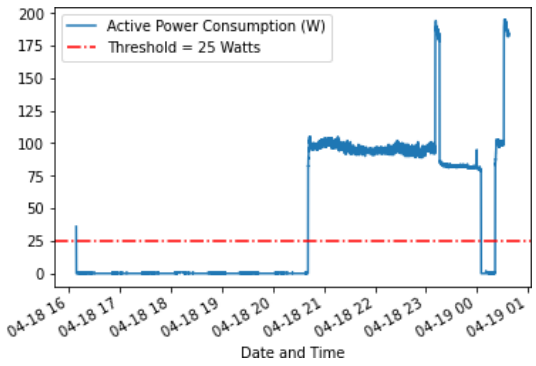

Figure 4. Example of power observations data plotted against time with the threshold value dividing the power values into two groups: values above the threshold represent an ON state, while the rest represent an OFF state.

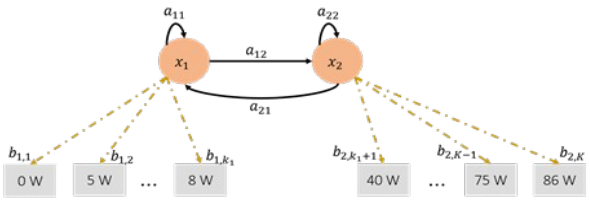

Figure 5. A diagram showing the emission probabilities connecting a mutually exclusive set of observations to their respective states.

B. Model Generation

Although the math involved in calculating the model parameters is rather simple, the coding process itself requires multiple manipulations. Afterward, the model can be easily found and tested using the Viterbi algorithm. The manipulations are explained with their relative steps to provide the reader with context.

The input dataset is a time-series observation sequence $O = \{o_1, o_2, \ldots, o_T\}$ of length T. The flow of the created code (for model generation and testing) is summarized in the following steps:

Model Generation:

1) Convert the input (time-series) to a DataFrame type.
2) Define the state boundary (threshold), the number of states, and the initial probability vector (π).
3) Map the observations to their respective states (obtain state sequence).
4) Calculate the transition matrix.
5) Calculate the emission matrix.

Model Testing:

1) Generate a state sequence from the calculated model λ using the Viterbi algorithm.
2) Use the accuracy metric to verify the model.

TABLE I. DEFINED PARAMETERS OF THE HMM MODEL BASED ON HUMAN OBSERVATIONS

parameter	Size	Description
State boundary	1 × 1	Threshold that separates between states
States (X)	1 × 2	Contains the FSM of the lamp. x_1 = OFF, x_2 = ON
Initial probability vector (π)	1 × 2	The probability of each state at zero time-step

1) Defining parameters: First, the power consumption data of the lamp is plotted to ensure that the data includes the entire FSM of the appliance. From Fig. 4, which shows the power consumption of a lamp for a period of nine hours (i.e., 8000 instants), we can see that the data includes two levels of power which represent the two states of the appliance. Moreover, the threshold that separates one state from the other is set to be 25 Watts based on the study conducted by [15]. Finally, the initial probability vector is decided based on our previous assumption. Table I summarizes the outputs of this step.

2) Mapping observations to states: This step is done using the state boundary. Any power value existing at or above the boundary is translated to state 1 (ON) and the rest is mapped to state 0 (OFF) as shown in Fig. 6. The state sequence will be used to find A and B.

3) Calculate the transition matrix (A): The transition matrix is calculated and verified using (1) and (2), respectively. A depiction of the results is provided in Fig. 7.

4) Calculate the emission matrix (B): The emission matrix is found using two steps. First, the frequency of zeros and ones are obtained from the state sequence. Second, the frequency of the power readings in the observation sequence is found. If the observation belongs to state zero or state one, then the frequency of that observation is divided by the frequency of the state it belongs to. Fig. 8 shows a sample of the total emission matrix (K = 50) where the sum of the emissions of a certain state is one. Now the model $\lambda = (\pi, A, B)$ is complete and ready to be tested.

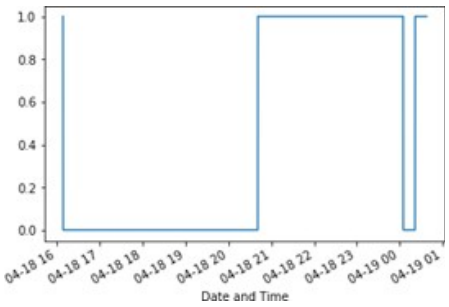

Figure 6. The sequence of states mapped from the original observation sequence of the lamp shown in Fig. 4.

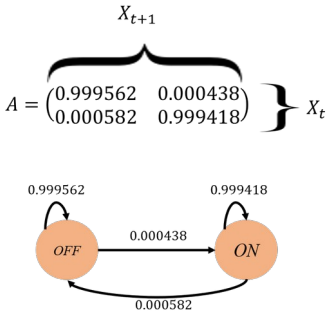

Figure 7. The transition matrix of the lamp model with the diagram depiction. It is showing that the summation of each row of the matrix (or the arrows coming out of a circle) is equal to one.

C. Viterbi Algorithm

The Viterbi algorithm, developed by A. J. Viterbi [16], is a dynamic programming technique that is used to solve the decoding problem of any HMM. The decoding problem states that given an observation sequence O and a model λ, the best sequence of the hidden states (ON or OFF) can be found using dynamic programming techniques (e.g., the Viterbi algorithm).

The goal of the Viterbi algorithm is to find the best path of states (starting from the last state) out of all the possible sequences in an efficient manner. If this procedure is done

conventionally, the statistical algorithm would have to go through $N^T = 2^{8000}$ sequences to find the best path. However, the Viterbi algorithm reduces that to $N^2 \times T = 2^2 \times 8000 \approx 2^{15}$.

To implement the Viterbi algorithm, three main steps are required: 1) Initialization, 2) Recursion, and 3) Termination [17], [18], [19].

	0.0 W	1.0 W	2.0 W	36.0 W	79.0 W	80.0 W	81.0 W	82.0 W	...	$\sum_{k=1}^{K} b_{ik}$
x_1	0.916466	0.083534	0.000291	0.0	0.0	0.0	0.0	0.0		1
x_2	0.0	0.0	0.0	0.000291	0.001454	0.009305	0.034894	0.085781		1

Figure 8. Sample of the results of the emission matrix of size $N \times K = 2 \times 50$

1) Model adaptation: Literature including [6], [9], and [10] claimed that constructing an averaged model from multiple appliance variants $\lambda_{avg} = ((\lambda_1 + \lambda_2 + \ldots + \lambda_m) \div m)$ improves the performance of the HMM when applied to a foreign appliance of the same type but with different power consumption levels. The authors mainly used laboratory-generated consumption data which does not necessarily represent the real-life application. Our study theorizes that the adaptation process will not be effective if there is a severe imbalance between the state transitions (i.e. a_{ii}, a_{jj} >> $a_{i,j}$, $a_{j,i}$; $i \neq j$ or vice versa).

Therefore, the same adaptation theory will be tested on the testing dataset. Equations (4) and (5) are used to adapt A and B, respectively.

$$A_{avg} = (\Sigma\, A_m) \div m;\ m = 3 \tag{4}$$

$$B_{avg} = (\Sigma\, B_m) \div m;\ m = 3 \tag{5}$$

Where m is the number of variants used for the adaptation process.

IV. Dataset Selection

The Reference Energy Disaggregation Dataset (REDD) and the Trace Base (TB) dataset were considered for testing the model-generating code. Both datasets provide a one-second resolution data of power consumed by home appliances. Table II shows the specification of each dataset [20]. The lamp's captured consumption in both datasets showcases fewer state alternations as shown in Fig. 9. Considering the different resolutions, we opted to select a data subset from the REDD solely while highlighting that they are similar in nature.

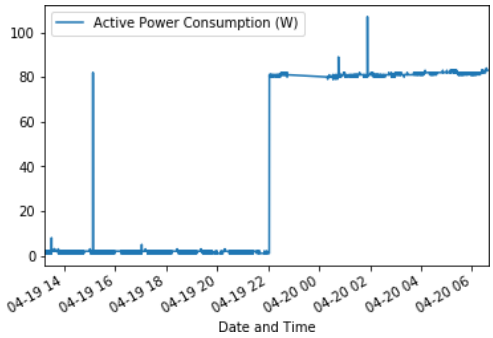

(a) Power consumed by a lamp from the REDD.

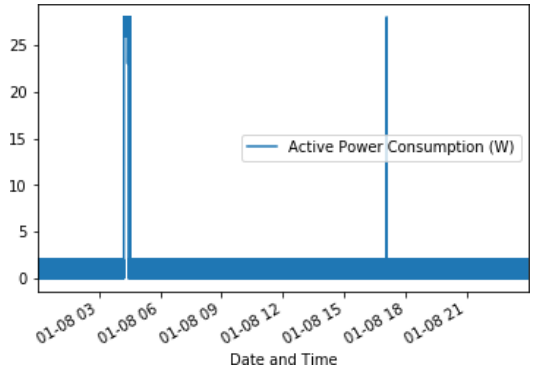

(b) Power consumed by a lamp from the TB dataset.

Figure 9. Depiction of the general trend observed in the state transition of lamps from REDD and TB. It shows that both datasets recorded similar behavior where there are fewer transitions from one state to another.

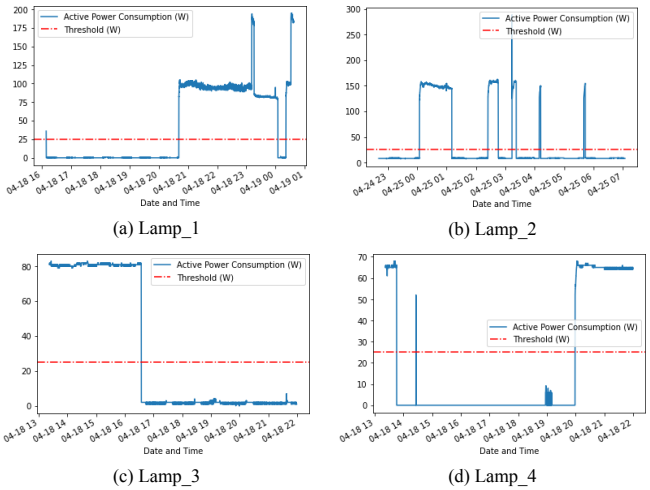

(a) Lamp_1 (b) Lamp_2

(c) Lamp_3 (d) Lamp_4

Figure 10. The complete observation sequence (i.e., nine hours of recording) for four different lamps, with a fixed state boundary at 25 Watts.

V. Methodology Testing

Before testing the adaptation theory, a single variant model was built to deduce the effect of data length and transitioning nature on the model's accuracy.

A. HMM for One Variant

An HMM model was developed for four distinct lamps from the REDD using 100%, 50%, and 25% of a specific

segment per lamp. A depiction of the entire segment of each lamp with a fixed state threshold is presented in Fig 10.

TABLE II. SPECIFICATIONS OF THE REDD AND THE TB DATASETS

	Tracebase (TB)	Reference Energy Disaggregation Dataset (REDD)
Resolution for Independent Circuits	Per one second, and eight seconds	Per three seconds
Country	Germany / Australia	United States of America
Number of Houses	N/A	Six
Type of Measurement	Individual circuits	Aggregated and individual circuits
Features	Active power	Current, voltage, and apparent power

B. Adapted HMM

The model adaptation is created to detect the hidden states (ON or OFF) of any lamp regardless of whether the model was trained on it previously or not. The performed test used three lamp variants for training (adapted using the average function) and one variant for testing as described in Table III.

VI. RESULTS AND DISCUSSION

The results were evaluated using the accuracy metric shown in (6) based on its prevalence in the previous literature.

$$\mathrm{Acc}(y, \hat{y}) = (1 \div n_{samples}) \times \Sigma 1(\hat{y_i} = y_i) \qquad (6)$$

Where $\hat{y}$ represents Viterbi generated sequence, and y represents the known state sequence.

A. HMM for One Variant

Table IV depicts the accuracy of each lamp at different lengths. At full length (8000 instants), lamp_2 gives the most accurate result. However, its performance trails off once the input data is reduced to half or a quarter of its original size. The 100% accuracy values stem from observing long periods of zero-state (OFF state) such as what is seen in Lamp_1 and Lamp_4. To further support the observation, we can see that the performance of Lamp_3 and Lamp_4 HMMs' deteriorate after cutting down the last half or three-quarters of the data, removing by that the long zero-state intervals. Furthermore, the model (λ) of Lamp_3 fails in generating an accurate state sequence for the first quarter where the sole observed state is an ON state which contradicts one of the assumptions stating that the input data must represent all the FSM of the appliance. Therefore, we deduce that prolonged OFF state induces high — and probably false — accuracy results; input data that does not represent the entire FSM of an appliance fails at generating a correct state sequence.

Table V examines the behavior of the four lamps. We observe that only one state exists in the shortest version of Lamp_3. Also, the data that shows better balance in state transitions are from Lamp_2 and Lamp_4 which are highlighted in green. Although both have similar balanced A matrices, Lamp_4 performed better in the accuracy test. We conclude from there that not only a balanced transition matrix is required to achieve high accuracy scores but also a diverse shape of input data (which does not include large chunks of zero-state observations), and a complete FSM representation.

TABLE III. THE COMBINATION OF THREE TRAINING VARIANTS USED TO TEST EACH APPLIANCE.

	Test Variants			
	Lamp_1	***Lamp_2***	***Lamp_3***	***Lamp_4***
Training Variants	Lamp_2, Lamp_3, Lamp_4	Lamp_1, Lamp_3, Lamp_4	Lamp_1, Lamp_2, Lamp_4	Lamp_1, Lamp_2, Lamp_3

TABLE IV. ACCURACY RESULTS (%) FOR THE FOUR DIFFERENT LAMPS AT DIFFERENT LENGTHS (INSTANTS).

	Accuracy (%)			
Length (instants)	***Lamp_1***	***Lamp_2***	***Lamp_3***	***Lamp_4***
8000	57.04	79.90	70.43	76.19
4000	100.00	65.55	40.85	100.00
2000	100.00	66.05	0.00	100.00

TABLE V. THE TRANSITION MATRIX, A, OF ALL LAMPS AT THREE DIFFERENT LENGTHS. THE OVERALL TREND SHOWS THAT THE PROBABILITY OF MAINTAINING A CERTAIN STATE FOR THE NEXT TIME STEP IS SIGNIFICANTLY GREATER THAN CHANGING ITS CURRENT STATE. HOWEVER, LAMPS THAT SHOW A BETTER PROBABILITY OF CHANGING THEIR STATE ARE HIGHLIGHTED IN GREEN.

		next state (j)							
		At a length of 8000 instants							
		Lamp_1		***Lamp_2***		***Lamp_3***		***Lamp_4***	
		OFF	**ON**	**OFF**	**ON**	**OFF**	**ON**	**OFF**	**ON**
current state (i)	**OFF**	0.999562	0.000438	0.999218	0.000782	1.000000	0.000000	0.999651	0.000349
	ON	0.000582	0.999418	0.003109	0.996891	0.000329	0.999671	0.000881	0.999119
		At a length of 4000 instants							
	OFF	1.000000	0.000000	0.999237	0.000763	1.000000	0.000000	0.999725	0.000275
	ON	1.000000	0.000000	0.001451	0.998549	0.000329	0.999671	0.005479	0.994521
		At a length of 2000 instants							
	OFF	1.000000	0.000000	0.999243	0.000757	0.000000	0.000000	0.999388	0.000612

	ON	1.000000	0.000000	0.000000	1.000000	0.000000	1.000000	0.005479	0.994521

B. *Adapted HMM*

Table VI shows the accuracy results produced by the four different tests conducted. The generated state sequences were approximate to the ones generated by the individual load models according to the accuracy results which indicates that the adapted model was successful.

The state sequence of Lamp_1 was decoded using an adaptive model (λ) constructed out of Lamp_2, Lamp_3, and Lamp_4. The accuracy results were slightly lower than the results generated by the HMM model of Lamp_1 itself. Moreover, we noticed that the length of the data does not impose a direct relationship on the accuracy results when tested. A Similar performance was observed in Lamp_4.

As for Lamp_2, the training variants were Lamp_1, Lamp_3, and Lamp_4. The adaptive model failed to generate a state sequence because the number of unique observations at 4000 and 2000 instants was less than the test appliance's observations. In other words, the observed power values at the test lamp were larger than what was provided by the adaptive model (λ). This fact further supports the findings of the single-variant models, stressing the diversity of the training model.

TABLE VI. THE ACCURACY RESULTS OF THE VITERBI STATE SEQUENCE GENERATED FOR FOUR TEST LAMPS USING AN ADAPTIVE HMM CONSTRUCTED OF THE THREE OTHER VARIANTS.

	Accuracy (%)			
Length	**Lamp 1**	**Lamp 2**	**Lamp 3**	**Lamp 4**
8000	53.96	78.91	62.93	72.49
4000	94.48	...	28.75	97.08
2000	89.00	...	9.3	94.15

In contrast, the adaptive model improved the accuracy of the shortest Lamp 3 observation sequence by 9.3%. However, this was not the case with the other two versions of the appliance.

VII. CONCLUSION

In this study, we successfully developed an HMM model from field-collected data to examine the methodology's validity. Both the one variant and adapted model achieved varied accuracy results. Based on our analysis, we deduced that the data nature (transitioning balance, and information quantity) plays a crucial role in the obtained results.

For future work, HMM can be integrated with other deep learning algorithms to enhance its performance especially when the input dataset is lacking shape diversity or suffering from a long duration of off-states. Also, the implementation of unsupervised learning methods for the parametrization procedure will drastically increase the versatility of the subsystem by enabling it to generate a model for more complex appliances such as dimming or multi-state appliances. Moreover, this will eliminate the cumbersome process of fine-tuning parameters manually. To take the subsystem a step further, an advanced algorithm can be used after the Viterbi algorithm to map the states (ON and OFF) to the actual power consumption series.

REFERENCES

[1] L. R. Rabiner, "A tutorial on hidden Markov models and selected applications in speech recognition," Proceedings of the IEEE, vol. 77, no. 2, pp. 257–286, Feb. 1989, conference Name: Proceedings of the IEEE.

[2] K. Ehrhardt-Martinez, K. A. Donnelly, S. Laitner et al., "Advanced metering initiatives and residential feedback programs: a meta-review for household electricity-saving opportunities." American Council for an Energy-Efficient Economy Washington, DC, 2010.

[3] Statista Research Department, "Saudi Arabia: electricity consumption by sector 2017," Aug. 2020. [Online]. Available: https://www.statista.com/statistics/710063/saudi-arabia-value-of-electricity-consumption-by-sector/

[4] B.-J. Yoon, "Hidden Markov Models and their Applications in Biological Sequence Analysis," Current Genomics, vol. 10, no. 6, pp. 402-415, Sep. 2009. [Online]. Available: https: //www.ncbi.nlm.nih.gov/pmc/articles/PMC2766791/

[5] T. Zia, D. Bruckner, and A. Zaidi, "A hidden Markov model based procedure for identifying household electric loads," in IECON 2011 - 37th Annual Conference of the IEEE Industrial Electronics Society. Melbourne, VIC, Australia: IEEE, Nov. 2011, pp. 3218-3223, iSSN: 1553-572X.

[6] J. A. Mueller, A. Sankara, J. W. Kimball, and B. McMillin, "Hidden Markov models for nonintrusive appliance load monitoring," in 2014 North American Power Symposium (NAPS). IEEE, Sep. 2014, pp. 1-6.

[7] A. Reinhardt, P. Baumann, D. Burgstahler, M. Hollick, H. Chonov,M. Werner, and R. Steinmetz, "On the accuracy of appliance identification based on distributed load metering data," in 2012 Sustainable Internet and ICT for Sustainability (SustainIT), Oct. 2012, pp. 1–9.

[8] L. Mauch, K. S. Barsim, and B. Yang, "How well can hmm model load signals," in Proceeding of the 3rd international workshop on non- intrusive load monitoring (NILM 2016), no. 6, 2016.

[9] A. Sankara, "Energy disaggregation in NIALM using hidden Markov models," Master's thesis, Missouri University of Science and Technology, Jan. 2015. [Online]. Available: https://scholarsmine.mst.e du/masters theses/7414

[10] P. Nandy, "Hidden Markov Model based non-intrusive load monitoring using active and reactive power consumption," Master's thesis, Missouri University of Science and Technology, Jan. 2016. [Online]. Available: https://scholarsmine.mst.edu/masters theses/7612

[11] Y. Ji, E. Buechler, and R. Rajagopal, "Data-Driven Load Modeling and Forecasting of Residential Appliances," IEEE Transactions on Smart Grid, vol. 11, no. 3, pp. 2652–2661, May 2020, conference Name: IEEE Transactions on Smart Grid.

[12] Pecan Street Inc., "Dataport from Pecan Street," 2017, austin, TX, USA. [Online]. Available: https://dataport.pecanstreet.org/

[13] R. V. Erickson, "Functions of Markov Chains," The Annals of Mathematical Statistics, vol. 41, no. 3, pp. 843–850, Jun. 1970. [Online]. Available: http://projecteuclid.org/euclid.aoms/1177696962

[14] L. C. G. Rogers and J. W. Pitman, "Markov Functions," The Annals of Probability, vol. 9, no. 4, pp. 573–582, Aug. 1981. [Online] Available:http://projecteuclid.org/euclid.aop/1176994363

[15] P. Delforge, S. Schmidt, and L. Schmidt, "Home Idle Load: Devices Wasting Huge Amounts of Electricity When Not in Active Use," May 2015. [Online]. Available: https://www.nrdc.org/sites/default/files/hom e-idle-load-IP.pdf

[16] A. J. Viterbi, "A Personal History of the Viterbi Algorithm," IEEE Signal Processing Magazine, vol. 23, no. 4, pp. 120–142, Jul. 2006, conference Name: IEEE Signal Processing Magazine.

[17] M. Burlando, “Hidden Markov Models — Part 2: the Decoding Problem,” Jan. 2019. [Online]. Available: https://medium.com/@Ayra Lux/hidden-markov-models-part-2-the-decoding-problem-c628ba474e69

[18] S. Teufel and A. Copestake, “Viterbi Algorithm for HMM Decoding,” University of Cambridge, 2017. [Online]. Available: https://www.cl.cam.ac.uk/teaching/1617/MLRD/slides/slides9.pdf

[19] D. Jurafsky and J. H. Martin, “Chapter A: Hidden Markov Model,” in Speech and Language Processing, 3rd ed., USA, Dec. 2020. [Online]. Available: https://web.stanford.edu/~jurafsky/slp3/A.pdf

[20] L. Pereira and N. Nunes, “Performance Evaluation in Non-Intrusive Load Monitoring: Datasets, Metrics, and Tools—A Review,” WIREs Data Mining and Knowledge Discovery, vol. 8, no. 6, p. e1265, 2018, eprint: https://onlinelibrary.wiley.com/doi/pdf/10.1002/widm.1265. [Online].